Published in final edited form as:
Dev Dyn. 2015 January ; 244(1): 86–97. doi:10.1002/dvdy.24185.

Selective Neuronal Lineages Derived from Dll4-Expressing Progenitors/Precursors in the Retina and Spinal Cord

Min Zou[1,4], **Huijun Luo**[1,3,4], and **Mengqing Xiang**[1,2,*]

[1]Center for Advanced Biotechnology and Medicine and Department of Pediatrics, Rutgers University-Robert Wood Johnson Medical School, 679 Hoes Lane West, Piscataway, New Jersey 08854, USA

[2]State Key Laboratory of Ophthalmology, Zhongshan Ophthalmic Center, Sun Yat-sen University, 54 South Xianlie Road, Guangzhou 510060, China

Abstract

Background—During retinal and spinal cord neurogenesis, Notch signaling plays crucial roles in regulating proliferation and differentiation of progenitor cells. One of the Notch ligands, Delta-like 4 (Dll4), has been shown to be expressed in subsets of retinal and spinal cord progenitors/precursors and involved in neuronal subtype specification. However, it remains to be determined whether Dll4 expression has any progenitor/precursor-specificity contributing to its functional specificity during neural development.

Results—We generated a *Dll4-Cre* BAC transgenic mouse line that drives Cre recombinase expression mimicking that of the endogenous Dll4 in the developing retina and spinal cord. By fate-mapping analysis, we found that Dll4-expressing progenitors/precursors give rise to essentially all cone, amacrine and horizontal cells, a large portion of rod and ganglion cells, but only few bipolar and Müller cells. In the spinal cord, Dll4-expressing progenitors/precursors generate almost all V2a and V2c cells while producing only a fraction of to few cells for other interneuron and motor neuron subtypes along the dorsoventral axis.

Conclusions—Our data suggest that selective expression of Dll4 in progenitors/precursors contributes to its functional specificity in neuronal specification and that the *Dll4-Cre* line is a valuable tool for gene manipulation to study Notch signaling.

Keywords

Dll4; Notch signaling; retina; spinal cord; V2 interneuron; neuronal lineage

INTRODUCTION

Notch signaling is an evolutionarily conserved intercellular mechanism essential for coordinating the proliferation and differentiation of multiple progenitors in a multitude of

*Corresponding author: Mengqing Xiang, Center for Advanced Biotechnology and Medicine, 679 Hoes Lane West, Piscataway, NJ 08854, Tel: 732-235-4491, Fax: 732-235-4466, xiang@cabm.rutgers.edu.
[3]Present address: Department of Biochemistry and Molecular Biology, Mayo Clinic Arizona, Scottsdale, Arizona 85259, USA.
[4]These authors contributed equally to this work.

organs and tissues during development (Gaiano and Fishell, 2002; Hitoshi et al., 2002; Murtaugh et al., 2003; Dontu et al., 2004; Sander and Powell, 2004; Nobta et al., 2005; Bolos et al., 2007; Laky and Fowlkes, 2008; Aguirre et al., 2010). In mammals, there are four Notch receptors (Notch1–4) and five Notch ligands named Jagged (Jag1 and Jag2) and Delta-like (Dll1, Dll3 and Dll4). Upon binding by a membrane-bound ligand on a neighboring cell, the Notch receptor undergoes proteolytic cleavages that cause the release of the Notch intracellular domain (NICD). The NICD then translocates into the nucleus of the recipient cell where it complexes with transcriptional coactivators to turn on the Notch effector genes (Oswald et al., 2001). During neural development, the Notch ligands and receptors are expressed in overlapping yet distinct patterns in central and peripheral nervous systems and play pivotal roles in the proliferation, maintenance, and differentiation of neural progenitors (Louvi and Artavanis-Tsakonas, 2006). For instance, Notch signaling is required for the maintenance of progenitor cells, specification of Müller cells, and inhibition of the photoreceptor cell fate during retinogenesis (Jadhav et al., 2006a; Jadhav et al., 2006b; Yaron et al., 2006; Hayes et al., 2007; Riesenberg et al., 2009; Nelson et al., 2011; Luo et al., 2012). In the developing ventral spinal cord, it is involved in progenitor maintenance and V2 interneuron subtype diversity (Yang et al., 2006a; Del Barrio et al., 2007; Peng et al., 2007; Kang et al., 2013). It appears that each Notch ligand may have a distinct role. For example, during inner ear development, Jag1 is crucial for establishing the prosensory domain whereas Dll1 and Jag2 act to limit hair cell production (Kiernan et al., 2005; Hartman et al., 2010). For retinal and spinal cord progenitors, Dll1 and Dll4 are both involved in their proliferation. While Dll1 appears to regulate neurogenesis in a domain-specific manner in the spinal cord (Marklund et al., 2010; Ramos et al., 2010), Dll4 is additionally required for generating neuronal diversity (Del Barrio et al., 2007; Rocha et al., 2009; Luo et al., 2012).

Dll4-mediated Notch signaling has been shown to be essential for vascular remodeling and arterial angiogenesis, T cell differentiation, and neural development (Liu et al., 2003; Corada et al., 2010; Billiard et al., 2011). In the spinal cord, Dll4 overexpression leads to increased V2b interneurons at the expense of V2a cells (Peng et al., 2007). It has been speculated that Dll4 may be preferentially expressed in V2a precursors to activate Notch signaling in neighboring V2b precursors for the specification of V2b interneurons (Del Barrio et al., 2007; Peng et al., 2007). The expression of Dll4 in a subset of progenitors/precursors in the V2 domain is consistent with this hypothesis (Rocha et al., 2009); however, to confirm it, one needs to demonstrate that Dll4-expressing progenitors/precursors selectively produce V2a interneurons. During retinal development, conditional ablation of Dll4 results in diminished progenitor proliferation and enhanced photoreceptor generation (Luo et al., 2012), implicating an important role for Dll4 in retinal cell type specification. As in the spinal cord, Dll4 and other Delta-like ligands Dll1 and Dll3 are expressed in subpopulations of retinal progenitors/precursors (Nelson et al., 2009). Just as well, it remains to be determined whether Dll4 expression has any progenitor/precursor-specificity commensurate with its function in cell type diversity.

Elucidating the neuronal lineages of Dll4-expressing progenitors/precursors will provide a cellular basis for understanding the Dll4-mediated Notch signaling events leading to cell type diversity in the retina and spinal cord. The transient nature of Dll4 expression precludes

a direct observation of Dll4 offspring. We thus utilized the Cre-loxP fate-mapping strategy to determine the cell lineages derived from Dll4-expressing progenitors/precursors in the retina and spinal cord. This allowed us to show that only selective cell types arise from Dll4-expressing progenitors/precursors during both retinal and spinal cord development, suggesting that preferential progenitor/precursor expression contributes to Dll4 functional specificity in cell type specification.

RESULTS

Dll4 Protein Expression Pattern during Retinal Development

To characterize the spatial and temporal expression pattern of Dll4 protein during mouse retinal development, we immunostained embryonic and postnatal retinas with a specific anti-Dll4 antibody. Dll4 immunoreactivity was first observed in a small population of progenitors/precursors in the central retina at E11.5 (Fig. 1A). Its expression then spread to increasing number of cells within the outer neuroblastic layer and by E13.5, the positive cells peaked and expanded to the entire retina (Fig. 1B). From E15.5 to P4, Dll4 expression remained in the outer neuroblastic layer but gradually decreased over time (Fig. 1C–E). Consistent with a previous report (Rocha et al., 2009), scattered Dll4 expression could also be detected in the RPE (retinal pigment epithelium) and vitreal space (Fig. 1A–E), which is most likely in red blood cells/vessels. At E15.5, some Dll4-expressing cells were found to be mitotic at S-phase as they could be pulse-labeled by EdU (Fig. 1F). In addition, a small number of Dll4-expressing cells could be colabeled by an antibody against phosphorylated histone H3, an M-phase marker (Fig. 1G). Thus, during mouse retinogenesis, Dll4 protein distributes in a pattern similar to that of *Dll4* RNA and the knocked-in *lacZ* reporter (Benedito and Duarte, 2005; Nelson et al., 2009). However, unlike a previous observation suggesting that Dll4 was expressed only in differentiating precursors (Rocha et al., 2009), we were able to show that Dll4 protein is expressed in mitotic retinal progenitors as well.

Generation of *Dll4-Cre* BAC Transgenic Mice

The subset of retinal precursors that express Dll4 could give rise to all or distinct retinal cell types. To distinguish these two possibilities, we determined the cell lineages of Dll4-expressing precursors by the Cre-loxP fate-mapping strategy. A BAC containing the mouse *Dll4* locus was modified by recombineering in *E. coli* to insert the Cre coding region at the Dll4 translation initiation site (Copeland et al., 2001; Gong et al., 2002; Warming et al., 2005; Yang et al., 2006b) (Fig. 2A). This modified BAC contains all the exons and introns of *Dll4* plus 114 kb 5′-flanking and 72 kb 3′ flanking sequences (Fig. 2A). Three transgenic founder lines were obtained for this *Dll4-Cre* BAC transgene with all lines displaying a similar Cre expression pattern.

When we crossed *Dll4-Cre* mice with the *R26R-YFP* or *-lacZ* strains (Soriano, 1999; Srinivas et al., 2001), we obtained embryos that exhibited reporter expression in the aorta, brain, eye, and spinal cord (Fig. 2B), in a pattern resembling that of β-gal expressed from *lacZ* knocked in the *Dll4* locus (Benedito and Duarte, 2005). A direct comparison of the *R26R-lacZ* reporter with *Z/EG* reporter revealed underreporting of *lacZ* expression in adult photoreceptors in a previous report (Feng et al., 2010). Meanwhile we also noticed a

dramatic lower expression of the *YFP* reporter within photoreceptors in postnatal retinas of *Dll4-Cre; R26R-YFP* mice, compared to that of the *GFP* reporter in *Dll4-Cre; Z/EG* mice (unpublished observation). Therefore, we crossed *Dll4-Cre* mice with the *Z/EG* strain (Novak et al., 2000) to perform unbiased lineage analysis in the retina. In the spinal cord, we did not detect any obvious difference in reporter expression patterns between *Dll4-Cre; R26R-YFP and Dll4-Cre; Z/EG* mice (Figs. 6–8) so we performed lineage analysis in the spinal cord using the *Dll4-Cre; R26R-YFP* animal.

In E13.5 retinas of *Dll4-Cre* transgenic embryos, double-immunolabeling showed that Cre and Dll4 proteins are co-expressed in many cells throughout retinal neuroblastic layer (Fig. 2C–E). Meanwhile, subsets of cells that express only Dll4 or Cre can also be detected (Fig. 2C–E). At the RNA level, *in situ* hybridization performed on adjacent sections revealed highly similar expression patterns of *Dll4* and *Cre* mRNA throughout the retina, although the expression level of *Cre* mRNA appears to be slightly lower than that of *Dll4* (Fig. 2O and P). In E12.5 *Dll4-Cre; Z/EG* embryos, Cre appears to colocalize with GFP in a subset of cells in the inner and outer neuroblastic layers (Fig. 2F–H), consistent with the expression of Dll4 in a subpopulation of progenitors/precursors (Fig. 1) (Luo et al., 2012). Similarly, in the ventral spinal cord of E10.75 *Dll4-Cre* embryos, Cre-expressing cells are located within the V2 domain in a position more lateral than Dll4-expressing cells (Fig. 2I–K), and Cre colocalizes with Dll4 only in a subset of cells (Fig. 2I–K). Meanwhile, *Dll4* and *Cre* mRNA appears to be located in the same V2 domain on adjacent sections although *Cre* expression level is lower than that of *Dll4* (Fig. 2Q and R). At E12.5 in *Dll4-Cre; R26R-YFP* embryos, Cre colocalizes with YFP in a group of cells within the V2 domain (Fig. 2L–N), in a pattern similar to that of the *lacZ* reporter knocked in the *Dll4* locus (Benedito and Duarte, 2005). Therefore, the *Dll4-Cre* BAC transgene is able to drive Cre expression in a spatiotemporal pattern closely mimicking that of the endogenous *Dll4* gene at least in the retina and spinal cord.

The notion that Dll4 and Cre proteins, and likewise Cre and GFP/YFP proteins are not completely colocalized in subsets of cells in the embryonic retina and spinal cord suggests possible temporal expression delays of Cre relative to Dll4, and GFP/YFP to Cre proteins, which is consistent with observed lower mRNA levels of *Cre* than *Dll4* in both the retina and spinal cord (Fig. 2O–R). The minor discrepancies between Cre and Dll4 expression could also result from the phenomenon of random monoallelic expression (Eckersley-Maslin and Spector, 2014). Furthermore, due to the known transient nature of Dll4 expression (Rocha et al., 2009), the discrepancy of Dll4 and Cre expression in subsets of cells may be caused by longer retention of Cre than Dll4 as well. Finally, the Cre-mediated recombination in the retina and spinal cord could be partial in some cells as we failed to observe complete colocalization between Cre and GFP/YFP proteins in both tissues (Fig. 2C–H), which could result from lower expression of *Dll4* in those cells.

Cell Lineages of Dll4-Expressing Retinal Progenitors/Precursors

In *Dll4-Cre; Z/EG* retinas, Dll4-derived GFP^+ cells were detected within both inner and outer neuroblastic layers in central regions of the retina at E12.5 and E13.5 (Fig. 3A, B). From E12.5 to P8, GFP^+ cells expanded from central to peripheral regions of the retina, and

by P8, GFP$^+$ cells were detected in all layers of the retina (Fig. 3A–D). At E16.5, Pax6 colocalized with GFP in most cells of the inner nuclear layer but in the ganglion cell layer, the majority of Pax6$^+$ cells did not co-express GFP (Fig. 3E). Similarly, most of the Brn3b- or calbindin-immunoreactive cells in the ganglion cell layer were negative for GFP expression, whereas all calbindin-immunoreactive horizontal cells in the outer neuroblastic layer co-expressed GFP (Fig. 3F and G). Meanwhile, GFP-labeled cells were detected at the outer edge of the outer neuroblastic layer and most of them co-expressed Otx2, a marker for photoreceptors (Baas et al., 2000; Koike et al., 2007) (Fig. 3H). By P8, Dll4-expressing progenitors gave rise to many GFP$^+$ cells located in the outer nuclear layer, inner half of the inner nuclear layer, and ganglion cell layer (Fig. 3D), exhibiting a significant cell type-specificity. Co-immunostaining with antibodies against GFP and selected retinal markers indicated that at this stage, nearly all GFP$^+$ cells in the outer nuclear layer co-expressed recoverin or rhodopsin (Fig. 3I, J). In the outer part of the inner nuclear layer, all calbindin$^+$ horizontal cells appeared to co-express GFP (Fig. 3K). However, almost none of PKCα^+ bipolar cells were immunoreactive for GFP (Fig. 3L). In the ganglion cell layer, some calbindin$^+$ cells were co-labeled for GFP, while many of them were also negative for it (Fig. 3K).

At P21, nearly all Rxrg-immunoreactive cones were co-labeled for GFP (Fig. 4M and N), while about 71% of recoverin-immunoreactive rods and cones (Fig. 4K and N), and most rhodopsin-immunoreactive rods were co-labeled for GFP (Fig. 4L), indicating that Dll4-expressing precursors may contribute to a large portion of photoreceptor cells, and perhaps to all cones. Similarly, all or nearly all calbindin$^+$ or Lhx1/5$^+$ (Fig. 4C, D and N) horizontal cells and Gad65$^+$ or GLYT1$^+$ amacrine cells co-expressed GFP (Fig. 4F, G and N), suggesting that all amacrine and horizontal cells may be derived from Dll4-expressing precursors. In agreement, nearly all Bhlhb5$^+$ displaced amacrine cells in the ganglion cell layer co-expressed GFP (Fig. 4E and N). However, only about 53% of Brn3b$^+$ ganglion cells, 6% of Chx10$^+$ bipolar cells, and 4% of Sox9$^+$ Müller cells co-expressed GFP (Fig. 4B, H, I, and N). The low frequency of GFP detection in Müller cells was also revealed by non-colocalization of GFP and glutamine synthetase in those cells (Fig. 4J). The 72% colocalization between Pax6 and GFP was consistent with the lack of GFP expression in many ganglion cells (Fig. 4A and N). Similarly, about 74% of total Bhlhb5$^+$ cells were found immunoreactive for GFP, which is consistent with the lack of GFP expression in the great majority of bipolar cells (Fig. 4E and N). Thus, the Dll4 lineage displays a considerable specificity, implicating and consistent with cell-type specific functions for Dll4 during retinal development.

Cell Lineages of Dll4-Expressing Spinal Cord Progenitors/Precursors

During mouse embryogenesis, Dll4 initiates its expression in the marginal zone of both dorsal and ventral spinal cords at E9.5 (Benedito and Duarte, 2005). Starting from E10.5, Dll4 expression is gradually restricted to the p2/V2 domain in the ventral spinal cord, before being down-regulated in spinal cord neurons after E12.5 (Benedito and Duarte, 2005; Del Barrio et al., 2007; Peng et al., 2007; Rocha et al., 2009). Based on EdU pulse-labeling at E10.5, we found that some Dll4-expressing cells in the ventral spinal cord around the p2 domain were mitotic progenitors (Fig. 1H). To determine the subtypes of neurons derived

from Dll4-expressing cells in the spinal cord, we double-immunolabeled spinal cord sections from *Dll4-Cre; R26R-YFP* embryos with antibodies against YFP and a variety of spinal cord neuron markers. At E10.75, YFP^+ cells were found distributed in several domains along the marginal zone of the dorsal spinal cord (Fig. 5A–D). This temporal and spatial pattern of YFP^+ cells coincides with that of the early generated dorsal interneuron populations dI1-dI6 (Fig. 5A–D) (Helms and Johnson, 2003). Quantification of double-labeled cells showed that 26.8% of $Isl1/2^+$ cells in the dI3 domain (Fig. 5A, E), 18.4% of $Brn3a^+$ cells in the dI1, 2, 3, and 5 domains (Fig. 5B, E), 4.7% of $Lhx1/5^+$ cells in the dI2 domain (Fig. 5C, E), and 2.7% of $Lhx1/5^+$ and 0.5% of $Pax2^+$ cells in the dI4 domain (Fig. 5C–E) co-expressed YFP. These results suggest that Dll4 is transiently expressed in varying subsets of precursors to the dI1–6 interneurons, which is consistent with the observation that Dll4 is expressed in these domains at E9.5 (Benedito and Duarte, 2005).

During development of the ventral spinal cord, Dll4 expression is restricted to the p2/V2 domain after E10.5, and several lines of evidence suggest that Dll4 is involved in regulating the generation of V2a and V2b interneurons from a common progenitor pool (Benedito and Duarte, 2005; Del Barrio et al., 2007; Peng et al., 2007; Rocha et al., 2009; Misra et al., 2014). Indeed, we found that at E10.75 in the ventral spinal cord, the majority of YFP^+ cells were located adjacent but ventral to the V1 interneuron population marked by the expression of En1 (Moran-Rivard et al., 2001), and very few $En1^+$ cells were labeled for YFP (Fig. 6K, L).

By E12.5, a distinct population of YFP^+ cells can be detected to co-express Cre, and occupy a region lateral to the ventricular zone in the same domain as the subset of $Ascl1^+$ V2 progenitor population (Fig. 6A, B) (Li et al., 2005). The majority of YFP^+ cells were present in the mantle layers, spanning ventrally from the V2 domain to the floor plate (Fig. 6A–J), indicating that they are differentiated into certain types of ventral spinal cord interneurons and/or motor neurons. By double-immunolabeling, we found that nearly all $Sox1^+$ V2c cells (Panayi et al., 2010) and $Chx10^+$ V2a cells (Briscoe et al., 2000) co-expressed YFP (Fig. 6C, D, L), whereas only about 38% of $Gata2^+$ V2b cells (Karunaratne et al., 2002) did (Fig. 6E, L). YFP expression could also be detected in 60% of $Lhx3^+$ V2a and/or motor neurons (Tanabe et al., 1998) (Fig. 6F, L). By double-immunostaining with antibodies against Mnx1 or Isl1/2 (Pfaff et al., 1996; Arber et al., 1999), we confirmed YFP expression in a small population of motor neurons - about 9% of $Mnx1^+$ motor neurons were YFP^+ (Fig. 6G, H, L). In addition, about 4.5% of $Evx1^+$ V0 cells (Moran-Rivard et al., 2001) and 2.2% of $Nkx2.2^+$ V3 cells (Briscoe et al., 1999) were immunoreactive for YFP (Fig. 6I, J, L). These observations suggest that in the ventral spinal cord, Dll4-expressing progenitors/precursors give rise to almost all V2a and V2c cells, but only to a portion of V2b cells. Moreover, only a small fraction of motor neurons and very few V0, V1 and V3 cells are generated from Dll4-expressing progenitors/precursors.

We also examined the fate of Dll4-derived cells in the postnatal spinal cord, by double-immunostaining spinal cord sections from P10 *Dll4-Cre; R26R-YFP* animals with antibodies against YFP and neural or glial cell markers. At this stage, YFP^+ cells were sparsely distributed in the gray matter of the spinal cord, and a few YFP^+ cells were also seen in the white matter (Fig. 7A–C). Quantification of co-immunolabeled cells revealed that about

60.3% of YFP^+ cells were $NeuN^+$ neurons (Fig. 7A, D), 16.3% were $Olig2^+$ oligodendrocytes (Fig. 7B, D), and 6.7% were $GFAP^+$ (glial fibrillary acidic protein) astrocytes (Fig. 7C, D). These results suggest that in the spinal cord, most Dll4-expressing progenitors/precursors give rise to neurons while only a small proportion of them generate glial cells.

DISCUSSION

In this study, we traced the lineages of Dll4-expressing progenitors/precursors in the retina and spinal cord by generating a BAC transgenic mouse line (*Dll4-Cre*) that expresses Cre recombinase for Cre-loxP fate-mapping. We determined the cell types for the offspring of Dll4-expressing cells by crossing the *Dll4-Cre* mice with the *Z/EG* and *R26R-YFP*/*lacZ* reporter lines followed by immunostaining analyses with antibodies against GFP/YFP and cell type-specific markers. These experiments have led to the conclusion that only selective cell types arise from Dll4-expressing progenitors/precursors during both retinal and spinal cord development, thereby suggesting a cellular mechanism for Dll4 functional specificity in cell type specification.

In the retina, we found that Dll4-expressing progenitors/precursors give rise to essentially all amacrine and horizontal cells and the majority of photoreceptors. On the other hand, only about half of Brn3b-expressing ganglion cells are derived from Dll4-expressing progenitors/precursors, and these progenitors/precursors produce very few bipolar and Müller cells. These observations are in agreement with the expression pattern of Dll4 in the developing retina, which is predominately localized to the outer neuroblastic layer at embryonic stages. Furthermore, our results are consistent with a previous report, in which the fates of retinal cells expressing *Dll4* were roughly examined by analyzing β-gal expression in a $Dll4^{LacZ/+}$ strain (Rocha et al., 2009), and were found to include amacrine, horizontal, ganglion, and photoreceptor cells. Nonetheless, the relatively short β-gal perdurance limited the accuracy and completeness of the mapping result. Our fate-mapping study based on the Cre-loxP system was able to provide an accurate and quantitative analysis of all the cell lineages derived from Dll4-expressing retinal progenitors/precursors.

In the spinal cord, we found that Dll4-expressing progenitors/precursors preferentially give rise to V2 cell lineages while generating a small number to few cells for all other interneuron and motor neuron subtypes along the dorsoventral axis, providing an explanation for the predominant role identified thus far for Dll4 in the binary V2 cell fate specification (Del Barrio et al., 2007; Peng et al., 2007; Misra et al., 2014). Similar to those in the retina, Dll4-expressing progenitors/precursors in the spinal cord generate mostly neuronal offspring and only a small number of oligodendrocytes and astrocytes, two glial cell types.

In the V2 domain of the spinal cord, we found that nearly all $Chx10^+$ V2a and $Sox1^+$ V2c neurons are generated from Dll4-expressing progenitors/precursors and only about 38% of $Gata2^+$ V2b neurons are derived from them. Moreover, early V2b precursors have been shown to lack Dll4 expression (Misra et al., 2014). These observations are in line with our current understanding of how Notch signaling is involved in regulating the diversification of

V2a and V2b subtypes from p2 progenitors. It has been proposed that V2a and V2b neurons are generated from common progenitor cells that express a combination of transcription factors including Lhx3, Gata2, Ascl1, and Foxn4. Dll4 expressed by V2a progenitors/precursors activates Notch signaling in V2b progenitors/precursors and non-autonomously promotes the V2b fate, while low or no Notch activity in V2a progenitors/precursors results in the generation of V2a cells autonomously (Li et al., 2005; Del Barrio et al., 2007; Peng et al., 2007). Consistent with this idea, our results indicated that Dll4 is preferentially expressed by V2a and only in subsets of V2b progenitors/precursors.

To characterize the lineages of Dll4-expressing progenitors/precursors in the retina and spinal cord, we created a BAC *Dll4-Cre* transgenic mouse line that can drive Cre recombinase expression in specific populations of neuronal progenitors/precursors during mouse embryogenesis, in a spatial and temporal pattern mimicking that of the endogenous Dll4. Thus, our *Dll4-Cre* transgenic line may also provide a useful tool for Cre-loxP-mediated conditional gain- and/or loss-of-function studies in the retina and spinal cord.

EXPERIMENTAL PROCEDURES

Mouse Strains and Generation of Transgenic Mice by BAC Recombineering

R26R-YFP (stock number: 006148), *R26R-LacZ* (stock number: 003474) and *Z/EG* (stock number: 004178) mice were purchased from The Jackson Laboratory (Bar Harbor, Maine).

A mouse BAC clone containing the *Dll4* locus (clone ID: RP23-468P3) was purchased from the BACPAC Resource Center (Children's Hospital Oakland Research Institute, Oakland, California). BAC recombineering was performed following a method described previously (Yang et al., 2006b). Briefly, a 1.46 kb fragment of *Dll4* promoter region (from −1462 bp to −1 bp upstream of the translation start site ATG) was amplified by PCR (primers used: 5′GGGAAAGCAGCTGCAGGGTTTG and 5′CCCTTGGGGTGTCCTCTCCACTC) and cloned into the PSC-A cloning vector (Catalog #240205, Agilent Technologies), then a Cre-SV40 PolyA cassette, generated from the pCAG-Cre plasmid (for Cre) (Addgene plasmid 13775) and pcDNA3.1 (for SV40 PolyA) (Life Technologies), was ligated downstream of the 1.46 kb *Dll4* promoter sequence. The Dll4-Cre-SV40 PolyA cassette was subsequently transferred into the plasmid pLD53.SCA-E-B (from Dr. Nathaniel Heintz, Rockefeller University, Sal I and Pac I digested) to obtain the plasmid construct PLD53-Dll4-Cre-SV40 PolyA. Meanwhile, the pSV1 vector (from Dr. Nathaniel Heintz, Rockefeller University) which contains a RecA recombinase gene, tetracycline resistance gene, and a temperature-sensitive replication origin was transformed into the bacteria strain DH10B containing the *Dll4* BAC clone. The transformed bacteria were grown on LB agar plates containing chloramphenicol (25 mg/ml) and tetracycline (5 mg/ml) at 30°C. These cells were subsequently transformed with the PLD53-Dll4-Cre-SV40 PolyA plasmid, grown at 30°C for 48 hrs, then spread on LB agar plates containing chloramphenicol (25 mg/ml) and ampicillin (50 mg/ml). The plate was incubated overnight at 43°C to screen for recombined clones by PCR. Correctly recombined BAC clone was amplified and purified for pronuclear microinjection (C57BL/6JxCBA F1 zygotes) at the transgenic/knockout core facility of the Rutgers Cancer Institute of New Jersey. PCR primers used to genotype *Dll4-Cre* transgenic mice are: 5′ AGGACACGTACTTAGAGCAG and 5′ CCGCATAACCAGTGAAACAGC.

X-Gal Staining, EdU Labeling, In Situ Hybridization, and Immunofluorescence

X-Gal (5-bromo-4-chloro-3-indolyl-β-D-galactopyranoside) staining of whole-mount embryos was carried out as described previously (Li et al., 2002; Li et al., 2004b). For EdU labeling, the Click-iT EdU labeling kit was purchased from Invitrogen. Timed pregnant mice were injected with EdU solution (30μg/g body weight) and pulse-labeled for 1.5 hrs. Staining was performed according to the protocol provided by the kit. RNA in situ hybridization was carried out as described previously (Mo et al., 2004). Digoxigenin-labeled riboprobes were prepared following the manufacturer's protocol (Roche Diagnostics). The probe for *Dll4* was described previously (Luo et al., 2012). The *Cre* probe was amplified by PCR from the PLD53-Dll4-Cre-SV40 PolyA construct according to previously described primers and sequence (Feng et al., 2009).

Staged mouse embryos were collected and fixed with 4% PFA/PBS and processed for cryosections. Immunofluorescent staining of cryosections was then carried out as previously described (Li et al., 2004a). The antibodies used in the immunostaining analysis are: anti-Dll4 (goat, 1:200, R&D systems, AF1389), anti-Pax6 [mouse, 1:100, Developmental Studies Hybridoma Bank (DSHB)], anti-Pax6 (rabbit, 1:5000, Chemicon, AB5409), anti-Gad65 (mouse, 1:1000, BD Pharmingen, 559931), anti-GLYT1 (goat, 1:5000, Chemicon, AB1770), anti-Brn3b (goat, 1:200, Santa Cruz Biotechnology, SC-6026), anti-calbindin (rabbit, 1:4000, SWANT, CB-38), anti-Chx10 (sheep, 1:1600, Exalpha Biologicals, X1180P), anti-recoverin (rabbit, 1:5000, Chemicon, AB5585), anti-rhodopsin (mouse, 1:1000, Sigma, R5403), anti-glutamine synthetase (mouse, 1:5000, Chemicon, MAB302), anti-PKCα (rabbit, 1:200, Cell Signaling, 2056S), anti-Rxrg (rabbit, 1:1000, Santa Cruz Biotechnology, SC-555), anti-Sox9 (rabbit, 1:1000, Chemicon, AB5535), anti-Lhx1/5 (mouse, 1:100, DSHB, 4F2), anti-Bhlhb5 (goat, 1:800, Santa Cruz Biotechnology, SC-6045), anti-Otx2 (goat, 1:1000, R&D systems, AF1979), anti-GFP (also for YFP) (goat, 1:1000, Abcam, AB6673), anti-GFP (also for YFP) (rabbit, 1:400, MBL International, JM-3999–100), anti-Cre (mouse, 1:1000, Covance, MMS-106P), anti-Gata2 (rabbit, 1:200, Santa Cruz Biotechnology, SC-9008), anti-Gata2 (guinea pig, 1:2000) (Peng et al., 2007), anti-Ascl1 (mouse, 1:100, BD Pharmingen, 556604), anti-Brn3a (mouse, 1:50, Chemicon, MAB1585), anti-Lhx3 (mouse, 1:100, DSHB, 67.4E12), anti-En1 (mouse, 1:25, DSHB, 4g11), anti-Evx1 (mouse, 1:100, DSHB, 99.1-3A2), anti-Mnx1 (mouse, 1:100, DSHB, 81.5c10), anti-Nkx2.2 (mouse, 1:50, DSHB, 74.5a5), anti-Isl1/2 (mouse, 1:50, DSHB, 39.4D5), anti-NeuN (mouse, 1:200, Chemicon, MAB377), anti-Olig2 (rabbit, 1:100) (Ligon et al., 2004), anti-GFAP (rabbit, 1:5000, DAKO, Z0334), and anti-Sox1 (guinea pig, 1:500) (Panayi et al., 2010). DAPI and TOPRO3 (Invitrogen) were used for nuclear counterstaining.

Quantification

To quantify marker-positive cells and cells co-expressing YFP/GFP and cell type-specific markers in the retina and spinal cord, at least three comparable embryos or postnatal mice of each type were counted for positively labeled cells on nonadjacent sections. Cells immunoreactive for dorsal interneuron markers (Isl1/2, Brn3a, Lhx1/5, and Pax2) were counted according to the distinct domains that they occupy at E10.75, when these domains are easily distinguishable (Helms and Johnson, 2003). The results were statistically analyzed.

Acknowledgments

Grant sponsor: NIH; Grant number: EY020849 and EY012020; Grant sponsor: New Jersey Commission on Spinal Cord Research; Grant number: 09-3087-SCR-E-0.

We thank Drs. David Rowitch and Stavros Malas for providing the anti-Olig2 and anti-Sox1 antibodies, respectively, Dr. Nathaniel Heintz for the pLD53.SCA-E-B and pSV1 plasmids, and Drs. Kamana Misra and Shengguo Li for thoughtful comments on the manuscript. This work was supported by the National Institutes of Health (EY020849 and EY012020 to M.X.), the New Jersey Commission on Spinal Cord Research (09-3087-SCR-E-0 to M.X.), and the 985 Project of the Ministry of Education of China (to M.X.).

References

Aguirre A, Rubio ME, Gallo V. Notch and EGFR pathway interaction regulates neural stem cell number and self-renewal. Nature. 2010; 467:323–327. [PubMed: 20844536]

Arber S, Han B, Mendelsohn M, Smith M, Jessell TM, Sockanathan S. Requirement for the homeobox gene *Hb9* in the consolidation of motor neuron identity. Neuron. 1999; 23:659–674. [PubMed: 10482234]

Baas D, Bumsted KM, Martinez JA, Vaccarino FM, Wikler KC, Barnstable CJ. The subcellular localization of Otx2 is cell-type specific and developmentally regulated in the mouse retina. Brain Res Mol Brain Res. 2000; 78:26–37. [PubMed: 10891582]

Benedito R, Duarte A. Expression of Dll4 during mouse embryogenesis suggests multiple developmental roles. Gene Expr Patterns. 2005; 5:750–755. [PubMed: 15923152]

Billiard F, Kirshner JR, Tait M, Danave A, Taheri S, Zhang W, Waite JC, Olson K, Chen G, Coetzee S, Hylton D, Murphy AJ, Yancopoulos GD, Thurston G, Skokos D. Ongoing Dll4-Notch signaling is required for T-cell homeostasis in the adult thymus. Eur J Immunol. 2011; 41:2207–2216. [PubMed: 21598246]

Bolos V, Grego-Bessa J, de la Pompa JL. Notch signaling in development and cancer. Endocr Rev. 2007; 28:339–363. [PubMed: 17409286]

Briscoe J, Pierani A, Jessell TM, Ericson J. A homeodomain protein code specifies progenitor cell identity and neuronal fate in the ventral neural tube. Cell. 2000; 101:435–445. [PubMed: 10830170]

Briscoe J, Sussel L, Serup P, Hartigan-O'Connor D, Jessell TM, Rubenstein JL, Ericson J. Homeobox gene *Nkx2.2* and specification of neuronal identity by graded Sonic hedgehog signalling. Nature. 1999; 398:622–627. [PubMed: 10217145]

Copeland NG, Jenkins NA, Court DL. Recombineering: a powerful new tool for mouse functional genomics. Nat Rev Genet. 2001; 2:769–779. [PubMed: 11584293]

Corada M, Nyqvist D, Orsenigo F, Caprini A, Giampietro C, Taketo MM, Iruela-Arispe ML, Adams RH, Dejana E. The Wnt/β-catenin pathway modulates vascular remodeling and specification by upregulating Dll4/Notch signaling. Dev Cell. 2010; 18:938–949. [PubMed: 20627076]

Del Barrio MG, Taveira-Marques R, Muroyama Y, Yuk DI, Li S, Wines-Samuelson M, Shen J, Smith HK, Xiang M, Rowitch D, Richardson WD. A regulatory network involving Foxn4, Mash1 and delta-like 4/Notch1 generates V2a and V2b spinal interneurons from a common progenitor pool. Development. 2007; 134:3427–3436. [PubMed: 17728344]

Dontu G, Jackson KW, McNicholas E, Kawamura MJ, Abdallah WM, Wicha MS. Role of Notch signaling in cell-fate determination of human mammary stem/progenitor cells. Breast Cancer Res. 2004; 6:R605–615. [PubMed: 15535842]

Eckersley-Maslin MA, Spector DL. Random monoallelic expression: regulating gene expression one allele at a time. Trends Genet. 2014; 30:237–244. [PubMed: 24780084]

Feng L, Xie ZH, Ding Q, Xie X, Libby RT, Gan L. MATH5 controls the acquisition of multiple retinal cell fates. Mol Brain. 2010; 3:36. [PubMed: 21087508]

Feng W, Simoes-de-Souza F, Finger TE, Restrepo D, Williams T. Disorganized olfactory bulb lamination in mice deficient for transcription factor AP-2ε. Mol Cell Neurosci. 2009; 42:161–171. [PubMed: 19580868]

Gaiano N, Fishell G. The role of notch in promoting glial and neural stem cell fates. Annu Rev Neurosci. 2002; 25:471–490. [PubMed: 12052917]

Gong S, Yang XW, Li C, Heintz N. Highly efficient modification of bacterial artificial chromosomes (BACs) using novel shuttle vectors containing the R6Kγ origin of replication. Genome Res. 2002; 12:1992–1998. [PubMed: 12466304]

Hartman BH, Reh TA, Bermingham-McDonogh O. Notch signaling specifies prosensory domains via lateral induction in the developing mammalian inner ear. Proc Natl Acad Sci U S A. 2010; 107:15792–15797. [PubMed: 20798046]

Hayes S, Nelson BR, Buckingham B, Reh TA. Notch signaling regulates regeneration in the avian retina. Dev Biol. 2007; 312:300–311. [PubMed: 18028900]

Helms AW, Johnson JE. Specification of dorsal spinal cord interneurons. Curr Opin Neurobiol. 2003; 13:42–49. [PubMed: 12593981]

Hitoshi S, Alexson T, Tropepe V, Donoviel D, Elia AJ, Nye JS, Conlon RA, Mak TW, Bernstein A, van der Kooy D. Notch pathway molecules are essential for the maintenance, but not the generation, of mammalian neural stem cells. Genes Dev. 2002; 16:846–858. [PubMed: 11937492]

Jadhav AP, Cho SH, Cepko CL. Notch activity permits retinal cells to progress through multiple progenitor states and acquire a stem cell property. Proc Natl Acad Sci U S A. 2006a; 103:18998–19003. [PubMed: 17148603]

Jadhav AP, Mason HA, Cepko CL. Notch 1 inhibits photoreceptor production in the developing mammalian retina. Development. 2006b; 133:913–923. [PubMed: 16452096]

Kang K, Lee D, Hong S, Park SG, Song MR. The e3 ligase mind bomb-1 (mib1) modulates delta-notch signaling to control neurogenesis and gliogenesis in the developing spinal cord. J Biol Chem. 2013; 288:2580–2592. [PubMed: 23223237]

Karunaratne A, Hargrave M, Poh A, Yamada T. GATA proteins identify a novel ventral interneuron subclass in the developing chick spinal cord. Dev Biol. 2002; 249:30–43. [PubMed: 12217316]

Kiernan AE, Cordes R, Kopan R, Gossler A, Gridley T. The Notch ligands DLL1 and JAG2 act synergistically to regulate hair cell development in the mammalian inner ear. Development. 2005; 132:4353–4362. [PubMed: 16141228]

Koike C, Nishida A, Ueno S, Saito H, Sanuki R, Sato S, Furukawa A, Aizawa S, Matsuo I, Suzuki N, Kondo M, Furukawa T. Functional roles of Otx2 transcription factor in postnatal mouse retinal development. Mol Cell Biol. 2007; 27:8318–8329. [PubMed: 17908793]

Laky K, Fowlkes BJ. Notch signaling in CD4 and CD8 T cell development. Curr Opin Immunol. 2008; 20:197–202. [PubMed: 18434124]

Li S, Misra K, Matise MP, Xiang M. Foxn4 acts synergistically with Mash1 to specify subtype identity of V2 interneurons in the spinal cord. Proc Natl Acad Sci U S A. 2005; 102:10688–10693. [PubMed: 16020526]

Li S, Mo Z, Yang X, Price SM, Shen MM, Xiang M. Foxn4 controls the genesis of amacrine and horizontal cells by retinal progenitors. Neuron. 2004a; 43:795–807. [PubMed: 15363391]

Li S, Price SM, Cahill H, Ryugo DK, Shen MM, Xiang M. Hearing loss caused by progressive degeneration of cochlear hair cells in mice deficient for the *Barhl1* homeobox gene. Development. 2002; 129:3523–3532. [PubMed: 12091321]

Li S, Qiu F, Xu A, Price SM, Xiang M. *Barhl1* regulates migration and survival of cerebellar granule cells by controlling expression of the neurotrophin-3 gene. J Neurosci. 2004b; 24:3104–3114. [PubMed: 15044550]

Ligon KL, Alberta JA, Kho AT, Weiss J, Kwaan MR, Nutt CL, Louis DN, Stiles CD, Rowitch DH. The oligodendroglial lineage marker OLIG2 is universally expressed in diffuse gliomas. J Neuropathol Exp Neurol. 2004; 63:499–509. [PubMed: 15198128]

Liu ZJ, Shirakawa T, Li Y, Soma A, Oka M, Dotto GP, Fairman RM, Velazquez OC, Herlyn M. Regulation of Notch1 and Dll4 by vascular endothelial growth factor in arterial endothelial cells: implications for modulating arteriogenesis and angiogenesis. Mol Cell Biol. 2003; 23:14–25. [PubMed: 12482957]

Louvi A, Artavanis-Tsakonas S. Notch signalling in vertebrate neural development. Nat Rev Neurosci. 2006; 7:93–102. [PubMed: 16429119]

Luo H, Jin K, Xie Z, Qiu F, Li S, Zou M, Cai L, Hozumi K, Shima DT, Xiang M. Forkhead box N4 (Foxn4) activates Dll4-Notch signaling to suppress photoreceptor cell fates of early retinal progenitors. Proc Natl Acad Sci U S A. 2012; 109:E553–562. [PubMed: 22323600]

Marklund U, Hansson EM, Sundstrom E, de Angelis MH, Przemeck GK, Lendahl U, Muhr J, Ericson J. Domain-specific control of neurogenesis achieved through patterned regulation of Notch ligand expression. Development. 2010; 137:437–445. [PubMed: 20081190]

Misra K, Luo H, Li S, Matise M, Xiang M. Asymmetric activation of Dll4-Notch signaling by Foxn4 and proneural factors activates BMP/TGFβ signaling to specify V2b interneurons in the spinal cord. Development. 2014; 141:187–198. [PubMed: 24257627]

Mo Z, Li S, Yang X, Xiang M. Role of the *Barhl2* homeobox gene in the specification of glycinergic amacrine cells. Development. 2004; 131:1607–1618. [PubMed: 14998930]

Moran-Rivard L, Kagawa T, Saueressig H, Gross MK, Burrill J, Goulding M. Evx1 is a postmitotic determinant of V0 interneuron identity in the spinal cord. Neuron. 2001; 29:385–399. [PubMed: 11239430]

Murtaugh LC, Stanger BZ, Kwan KM, Melton DA. Notch signaling controls multiple steps of pancreatic differentiation. Proc Natl Acad Sci U S A. 2003; 100:14920–14925. [PubMed: 14657333]

Nelson BR, Hartman BH, Ray CA, Hayashi T, Bermingham-McDonogh O, Reh TA. Acheate-scute like 1 (Ascl1) is required for normal delta-like (Dll) gene expression and notch signaling during retinal development. Dev Dyn. 2009; 238:2163–2178. [PubMed: 19191219]

Nelson BR, Ueki Y, Reardon S, Karl MO, Georgi S, Hartman BH, Lamba DA, Reh TA. Genome-wide analysis of Müller glial differentiation reveals a requirement for Notch signaling in postmitotic cells to maintain the glial fate. PLoS One. 2011; 6:e22817. [PubMed: 21829655]

Nobta M, Tsukazaki T, Shibata Y, Xin C, Moriishi T, Sakano S, Shindo H, Yamaguchi A. Critical regulation of bone morphogenetic protein-induced osteoblastic differentiation by Delta1/Jagged1-activated Notch1 signaling. J Biol Chem. 2005; 280:15842–15848. [PubMed: 15695512]

Novak A, Guo C, Yang W, Nagy A, Lobe CG. Z/EG, a double reporter mouse line that expresses enhanced green fluorescent protein upon Cre-mediated excision. Genesis. 2000; 28:147–155. [PubMed: 11105057]

Oswald F, Tauber B, Dobner T, Bourteele S, Kostezka U, Adler G, Liptay S, Schmid RM. p300 acts as a transcriptional coactivator for mammalian Notch-1. Mol Cell Biol. 2001; 21:7761–7774. [PubMed: 11604511]

Panayi H, Orford M, Panayiotou E, Genethliou N, Mean R, Lapathitis G, Li S, Xiang M, Kessaris N, Richardson WD, Malas S. SOX1 is required for the specification of a novel p2-derived interneuron subtype in the mouse ventral spinal cord. J Neurosci. 2010; 30:12274–12280. [PubMed: 20844123]

Peng CY, Yajima H, Burns CE, Zon LI, Sisodia SS, Pfaff SL, Sharma K. Notch and MAML signaling drives Scl-dependent interneuron diversity in the spinal cord. Neuron. 2007; 53:813–827. [PubMed: 17359917]

Pfaff SL, Mendelsohn M, Stewart CL, Edlund T, Jessell TM. Requirement for LIM homeobox gene *Isl1* in motor neuron generation reveals a motor neuron-dependent step in interneuron differentiation. Cell. 1996; 84:309–320. [PubMed: 8565076]

Ramos C, Rocha S, Gaspar C, Henrique D. Two Notch ligands, Dll1 and Jag1, are differently restricted in their range of action to control neurogenesis in the mammalian spinal cord. PLoS One. 2010; 5:e15515. [PubMed: 21124801]

Riesenberg AN, Liu Z, Kopan R, Brown NL. Rbpj cell autonomous regulation of retinal ganglion cell and cone photoreceptor fates in the mouse retina. J Neurosci. 2009; 29:12865–12877. [PubMed: 19828801]

Rocha SF, Lopes SS, Gossler A, Henrique D. Dll1 and Dll4 function sequentially in the retina and pV2 domain of the spinal cord to regulate neurogenesis and create cell diversity. Dev Biol. 2009; 328:54–65. [PubMed: 19389377]

Sander GR, Powell BC. Expression of notch receptors and ligands in the adult gut. J Histochem Cytochem. 2004; 52:509–516. [PubMed: 15034002]

Soriano P. Generalized lacZ expression with the ROSA26 Cre reporter strain. Nat Genet. 1999; 21:70–71. [PubMed: 9916792]

Srinivas S, Watanabe T, Lin CS, William CM, Tanabe Y, Jessell TM, Costantini F. Cre reporter strains produced by targeted insertion of EYFP and ECFP into the *ROSA26* locus. BMC Dev Biol. 2001; 1:4. [PubMed: 11299042]

Tanabe Y, William C, Jessell TM. Specification of motor neuron identity by the MNR2 homeodomain protein. Cell. 1998; 95:67–80. [PubMed: 9778248]

Warming S, Costantino N, Court DL, Jenkins NA, Copeland NG. Simple and highly efficient BAC recombineering using galK selection. Nucleic Acids Res. 2005; 33:e36. [PubMed: 15731329]

Yang X, Tomita T, Wines-Samuelson M, Beglopoulos V, Tansey MG, Kopan R, Shen J. Notch1 signaling influences V2 interneuron and motor neuron development in the spinal cord. Dev Neurosci. 2006a; 28:102–117. [PubMed: 16508308]

Yang Z, Jiang H, Chachainasakul T, Gong S, Yang XW, Heintz N, Lin S. Modified bacterial artificial chromosomes for zebrafish transgenesis. Methods. 2006b; 39:183–188. [PubMed: 16828309]

Yaron O, Farhy C, Marquardt T, Applebury M, Ashery-Padan R. Notch1 functions to suppress cone-photoreceptor fate specification in the developing mouse retina. Development. 2006; 133:1367–1378. [PubMed: 16510501]

Bullet points

- A *Dll4-Cre* BAC transgenic mouse line was generated that expresses Cre in a pattern mimicking that of the endogenous Dll4 in the developing retina and spinal cord.
- In the retina, Dll4-expressing progenitors/precursors give rise to essentially all cone, amacrine and horizontal cells, a large portion of rod and ganglion cells, but only few bipolar and Müller cells.
- Along the dorsoventral axis of the spinal cord, Dll4-expressing progenitors/precursors generate almost all V2a and V2c cells while producing only a fraction of to few cells for other interneuron and motor neuron subtypes.
- Selective expression of Dll4 in neuronal progenitors/precursors likely contributes to its functional specificity during neural development.

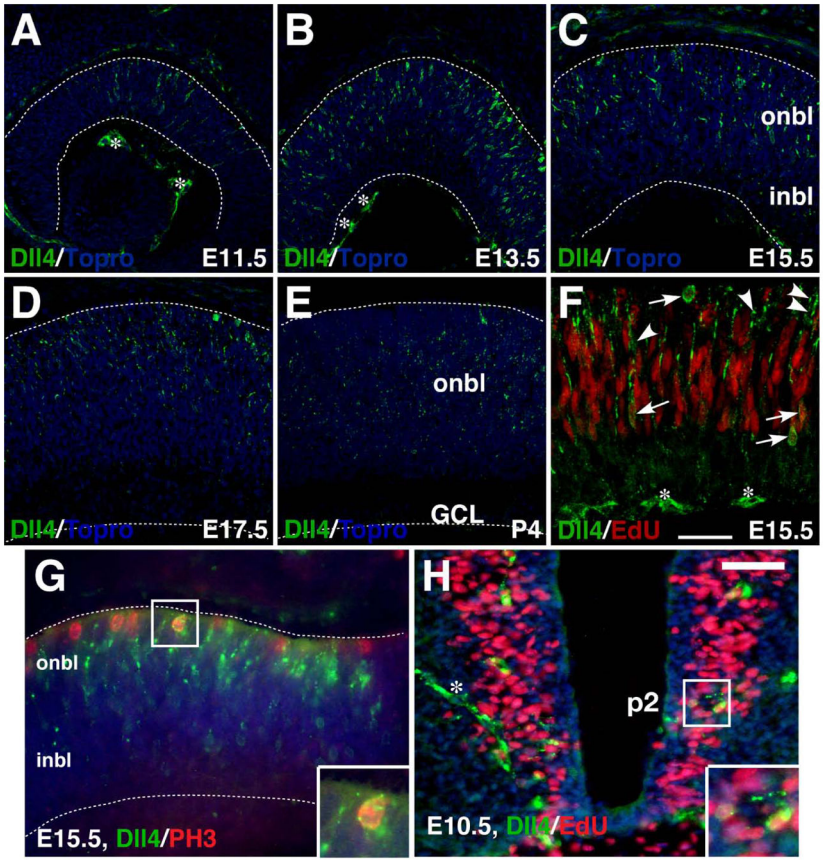

Fig. 1.

Expression of Dll4 protein in the developing retina and spinal cord. **A–E:** Retinal sections from the indicated stages were immunostained with an anti-Dll4 antibody (green), with nuclei counterstained with Topro (blue). The expression of Dll4 starts at E11.5 in the central retina, peaks at E13.5, and remains in the outer neuroblastic layer from E15.5 to P4. **F:** A retinal section from an E15.5 embryo pulse-labeled with EdU was both chemically stained for EdU (red) and immunostained with an anti-Dll4 antibody (green). Arrows point to representative colocalized cells while arrowheads point to representative cells labeled only for Dll4. **G:** An E15.5 retinal section was co-immunostained by antibodies against Dll4 and phosphorylated histone H3 (PH3). Note that Dll4 colocalizes with PH3 in scattered cells located at the outer edge of the onbl. **H:** An EdU pulse-labeled E10.5 spinal cord section was immunostained by Dll4 antibody and chemically stained for EdU. Note that Dll4 colocalizes with EdU in scattered cells around the p2 domain of ventral spinal cord. The asterisks indicate Dll4-immunoreactive blood vessels. Insets show corresponding outlined regions with representative colocalized cells at a higher magnification. Dashed lines outline the thickness of the retina. Abbreviations: GCL, ganglion cell layer; inbl, inner neuroblastic layer; onbl, outer neuroblastic layer. Scale bar in F = 75 μm (A, B), 47.6 μm (D, E), 39.7 μm (C), and 26.5 μm (F); Scale bar in H = 33.3 μm (G) and 50 μm (H).

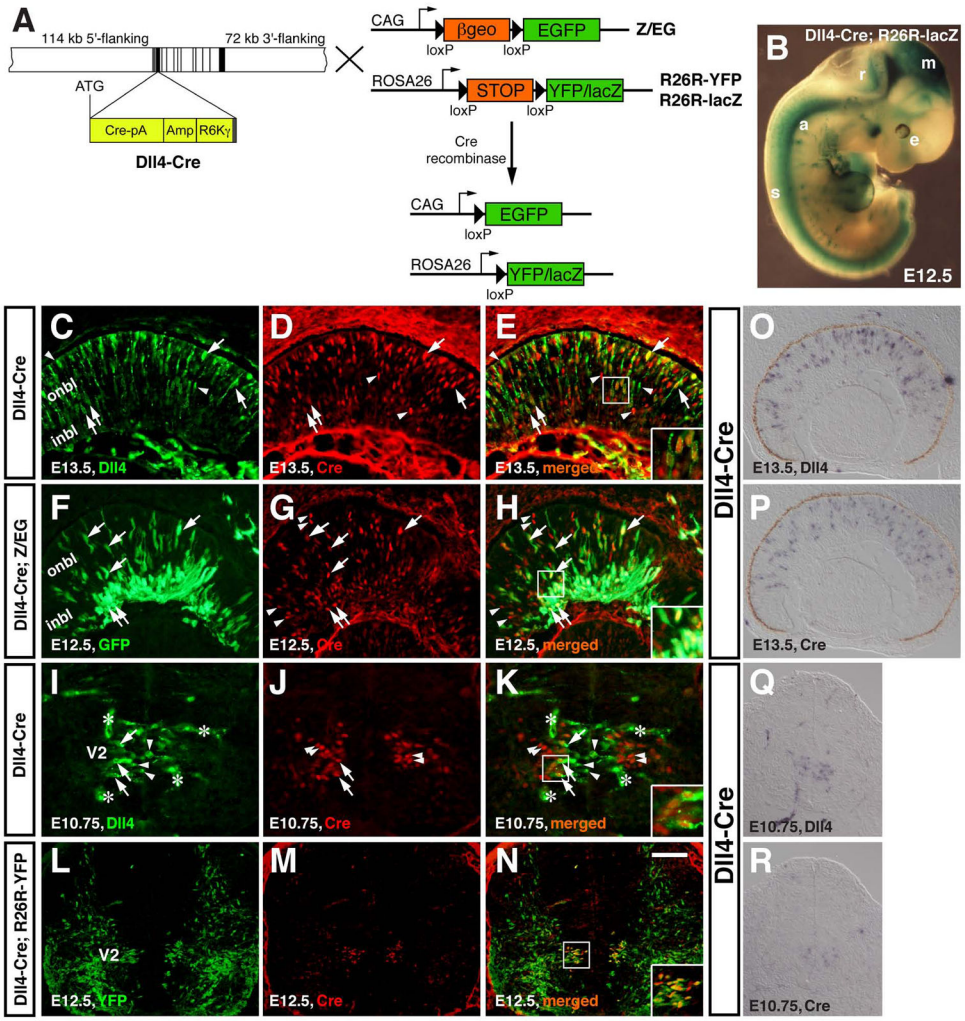

Fig. 2.

Generation of *Dll4-Cre* transgenic mice that express Cre recombinase in progenitors/precursors of the retina and spinal cord. **A:** The Cre-loxP system for conditional activation of reporter *YFP/lacZ* or *GFP* expression using *Dll4-Cre* and *R26R-YFP/lacZ* or *Z/EG* mice. To generate the *Dll4-Cre* BAC, a BAC containing the *Dll4* locus was modified by recombineering to insert the *Cre* coding region (Cre-pA) at the Dll4 translation initiation site (ATG), followed by the E. coli ampicillin resistance gene (*Amp*) and the *R6Kγ* origin for DNA replication. The exons are indicated by vertical black and gray bars and the estimated lengths of 5′-flanking and 3′ flanking sequences are also indicated. **B:** β-gal activity was visualized by X-gal staining in an E12.5 *Dll4-Cre; R26R-lacZ* wholemount embryo. **C–E:** A retinal section from an E13.5 *Dll4-Cre* embryo was immunolabeled with antibodies against Dll4 and Cre. **F–H:** A retinal section from E12.5 *Dll4-Cre; Z/EG* embryo was immunostained with antibodies against GFP and Cre. **I–K:** A spinal cord section from an E10.75 *Dll4-Cre* embryo was immunolabeled with antibodies against Dll4 and Cre. **L–N:** A spinal cord section from E12.5 *Dll4-Cre; R26R-YFP* embryo was immunostained with antibodies against YFP and Cre. Arrows point to representative colocalized cells, arrowheads point to representative non-colocalized cells, and the asterisks in (I, K) indicate

Dll4-immunoreactive blood vessels. Insets show corresponding outlined regions at a higher magnification. **O–R:** RNA in situ hybridization was performed for detecting *Dll4* (O, Q) and *Cre* (P, R) expression on adjacent sections. Abbreviations: a, aorta; e, eye; inbl, inner neuroblastic layer; m, mesencephalon; onbl, outer neuroblastic layer; r, rhombencephalon; s, spinal cord; V2, V2 domain. Scale bar=125 μm (Q, R), 100 μm (L–P), and 50 μm (C–K).

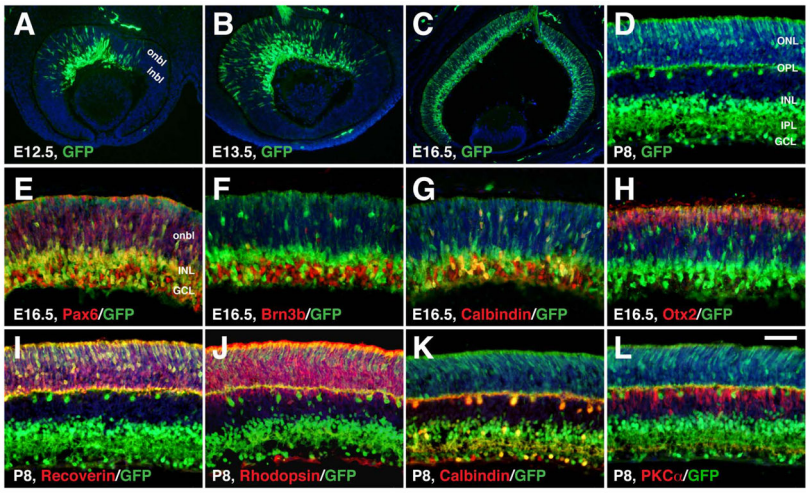

Fig. 3.

Selective retinal cell types derived from Dll4-expressing progenitors/precursors from E12.5 to P8. **A–L:** Retinal sections from *Dll4-Cre; Z/EG* mice at the indicated stages were immunostained with the indicated antibodies. Sections were counterstained with DAPI. Note the colocalization between GFP and Pax6, Brn3b, calbindin, Otx2, recoverin, or rhodopsin, but the absence of colocalization between GFP and PKCα. Abbreviations: GCL, ganglion cell layer; inbl, inner neuroblastic layer; INL, inner nuclear layer; IPL, inner plexiform layer; onbl, outer neuroblastic layer; ONL, outer nuclear layer; OPL, outer plexiform layer. Scale bar= 200 μm (C), 100 μm (A, B), and 50 μm (D–L).

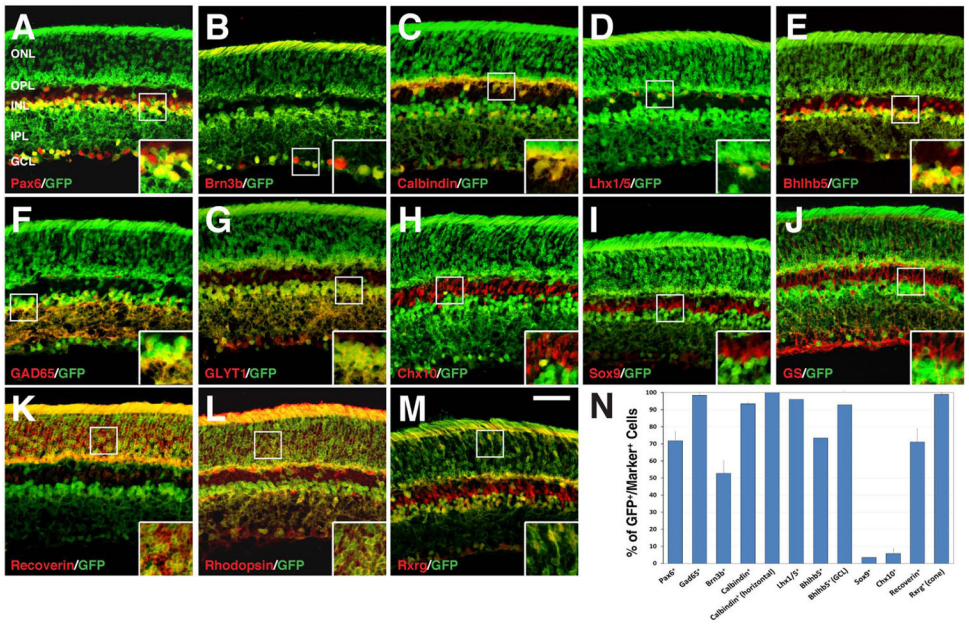

Fig. 4.

Retinal cell types derived from Dll4-expressing progenitors/precursors at P21. **A–M:** P21 retinal sections from *Dll4-Cre; Z/EG* mice were immunostained with the indicated antibodies. Insets show corresponding outlined regions at a higher magnification. Note the colocalization between GFP and Pax6, Brn3b, calbindin, Lhx1/5, Bhlhb5, GAD65, GLYT1, recoverin, rhodopsin, or Rxrg, but almost absence of colocalization between GFP and Chx10, Sox9, or GS (glutamine synthetase). **N:** Quantification of marker-immunoreactive cells that are positive for GFP in the *Dll4-Cre; Z/EG* retina. Each histogram represents the mean±SD for 3 retinas. Note that both total number of immunoreactive cells and immunoreactive cells within layers indicated in the parentheses were counted for calbindin, Bhlhb5 and Rxrg. Abbreviations: GCL, ganglion cell layer; INL, inner nuclear layer; IPL, inner plexiform layer; ONL, outer nuclear layer; OPL, outer plexiform layer. Scale bar = 47.6 μm (A–M).

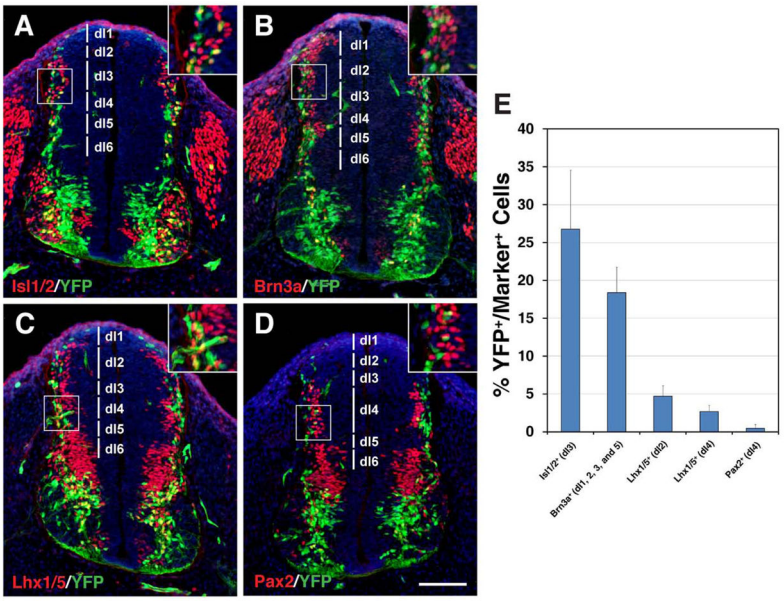

Fig. 5.

Dll4-expressing progenitors/precursors give rise to selective dorsal interneuron lineages in the spinal cord. **A–D**: Spinal cord sections from E10.75 *Dll4-Cre; R26R-YFP* embryos were stained by double-immunofluorescence using the indicated antibodies, as well as weakly counterstained with nuclear DAPI. Insets show corresponding outlined regions with representative colocalized cells at a higher magnification. YFP colocalizes with Isl1/2, Brn3a and Lhx1/5 but rarely with Pax2 in distinct domains (indicated by vertical lines) in the dorsal spinal cord. **E:** Percentages of dorsal interneuron marker-positive cells that are immunoreactive for YFP at E10.75. Each histogram represents the mean±SD for 3 different spinal cords. Note that each marker was counted within their distinct domains as indicated in the parentheses. Scale bar = 100 μm.

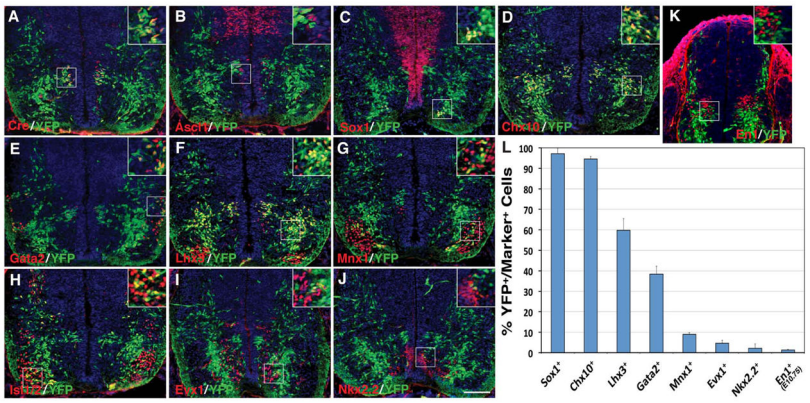

Fig. 6.

Selective ventral spinal cord cell types derived from Dll4-expressing progenitors/precursors. **A–K:** Spinal cord sections from E12.5 (A–J) or E10.75 (K) *Dll4-Cre; R26R-YFP* embryos were stained by double-immunofluorescence using the indicated antibodies as well as weakly counterstained with nuclear DAPI. Insets show corresponding outlined regions with representative colocalized cells at a higher magnification. Note that YFP colocalizes with Cre in many cells in the p2/V2 domain. YFP colocalizes also with Lhx3, Chx10, Gata2, Sox1, Mnx1, and Isl1/2 but rarely with Ascl1, Evx1, Nkx2.2 or En1 in distinct domains of the ventral spinal cord. **L:** Percentages of ventral neuron marker-positive cells that are immunoreactive for YFP at E12.5 or E10.75. Each histogram represents the mean±SD for 3 different spinal cords. Note that $En1^{+}$ cells were counted at E10.75 when these cells could be optimally labeled, and that Sox1-positive cells were counted only for those in the V2c domains but not for those in the ventricular zone. Scale bar = 100 μm.

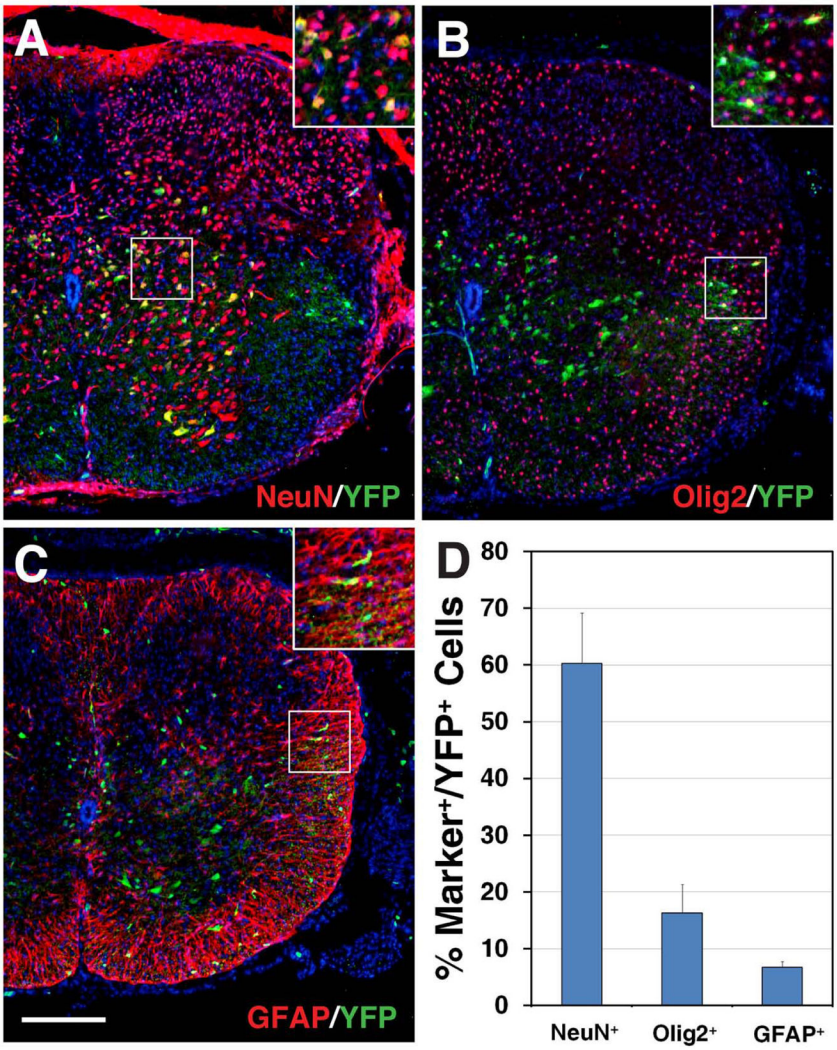

Fig. 7.

Detection of neural and glial cell lineages derived from Dll4-expressing progenitors/precursors in the postnatal spinal cord. **A–C:** Spinal cord sections from P10 *Dll4-Cre; R26R-YFP* mice were stained by double-immunofluorescence using the indicated antibodies as well as weakly counterstained with nuclear DAPI. Insets show corresponding outlined regions with representative colocalized cells at a higher magnification. Note that YFP colocalizes with NeuN in many cells within the gray matter (A), but with Olig2 and GFAP in much fewer cells in the white matter of the spinal cord (B and C). **D:** Percentages of YFP-positive cells that are immunoreactive for NeuN, Olig2 or GFAP at P10. Each histogram represents the mean±SD for 3 different spinal cords. Scale bar = 200 μm.

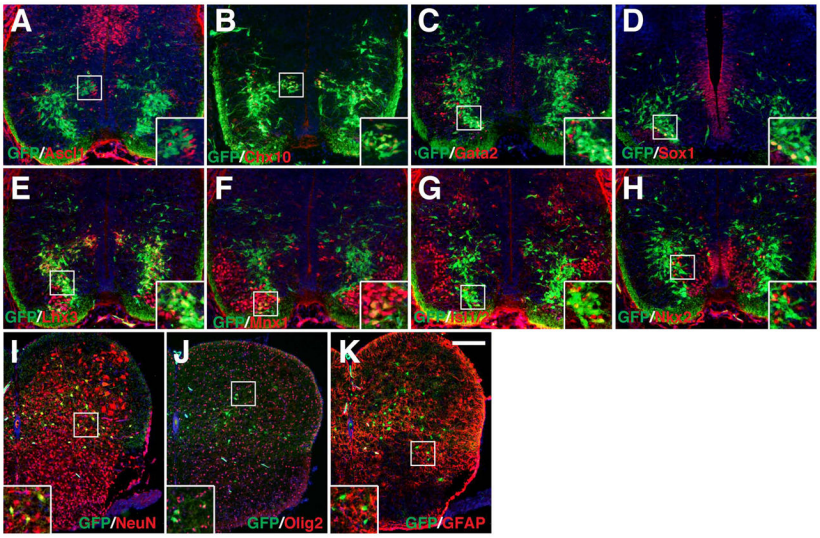

Fig. 8.

Selective spinal cord neural and glial cell types derived from Dll4-expressing progenitors/precursors in *Dll4-Cre; Z/EG mice*. **A–H:** Spinal cord sections from E12.5 *Dll4-Cre; Z/EG* embryos, except for panel **D**, which was at E13.5, were stained by double-immunofluorescence using the indicated antibodies as well as weakly counterstained with nuclear DAPI. Note that many $Chx10^{+}$, $Gata2^{+}$, $Sox1^{+}$, or $Lhx3^{+}$ cells co-express GFP, but only a small fraction to few $Mnx1^{+}$, $Isl1/2^{+}$, $Nkx2.2^{+}$, or $Ascl1^{+}$ cells are also positive for GFP. **I–K:** Spinal cord sections from P10 *Dll4-Cre; Z/EG* mice were stained by double-immunofluorescence using the indicated antibodies as well as weakly counterstained with nuclear DAPI. Note that GFP colocalizes with NeuN in many cells, but with Olig2 and GFAP in much fewer cells. Insets show corresponding outlined regions with representative colocalized cells at a higher magnification. Scale bar= 200 μm (I–K) and 100 μm (A–H).